arXiv:2607.05369v2 [cs.RO] 23 Oct 2026

GaP: A Graph-as-Policy Multi-Agent Self-Learning Harness For Variational Automation (VA) Tasks

Kaiyuan Chen[3,*] Shuangyu Xie[3,*] Letian Fu[3] Justin Yu[3] William Pacini[3]
Sandeep Bajamahal[3] Hudson Kim[3] Jaimyn Drake[3] Daehwa Kim[3] Haoru Xue[3]
Jonathan Francis[1] Christian Juette[1] Peter Schaldenbrand[1] Muhammet Yunus Seker[1]
Ruwan Wickramarachchi[1] Uksang Yoo[3] Guanzhi Wang[2]
Adithyavairavan Murali[2] Balakumar Sundaralingam[2] S. Shankar Sastry[3]
Yuke Zhu[2] Linxi "Jim" Fan[2] Spencer Huang[2] Ken Goldberg[3]

[1] Bosch [2] NVIDIA [3] University of California, Berkeley [*] equal contribution

Project Website: https://graph-robots.github.io/gap

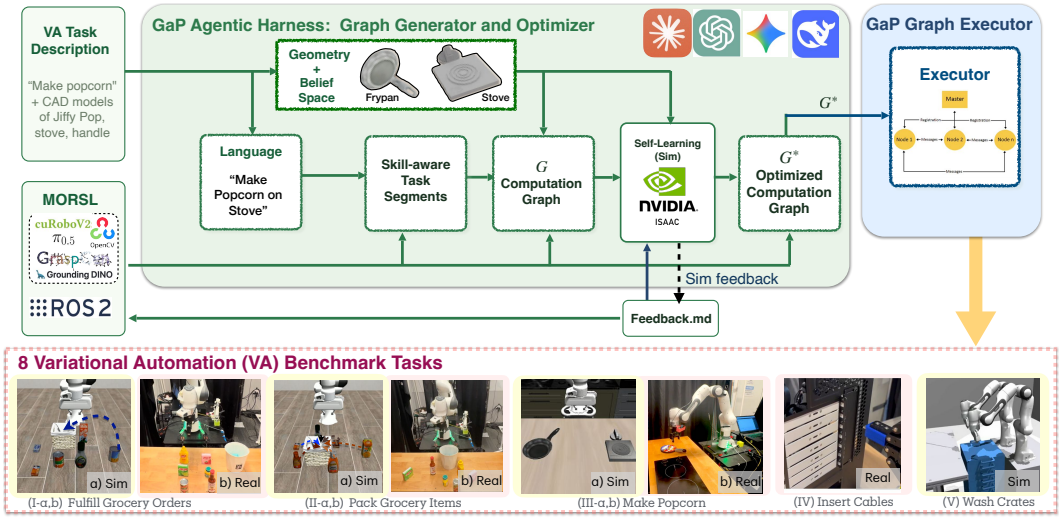


Figure 1: **GaP** system architecture. Given a "Variational Automation (VA)" task specification, GaP uses a multi-agent harness for coding agents such as Claude [1] and Gemini [2] to automatically generate computation graphs that include "skill" nodes from a Modular Open Robot Skill Library (MORSL), which includes model-based procedures (e.g. ROS [3]) and model-free policies (e.g. GraspGen [4]). GaP then orchestrates self-learning using simulation (e.g. Isaac Sim [5] and Newton [6]) to iteratively refine the graph, which can then be interpreted without the agents on an edge device for persistent execution over time. Bottom: 8 Variational Automation Benchmark Tasks (4 Sim and 4 Real).

Abstract: For robots to work reliably in commercial and industrial applications, recent advances in agentic coding systems have potential to combine interpretable robot programming with the open-world adaptability of model-free policies. We focus on "Variational Automation" (VA), a class of tasks that have larger variations in object geometry and pose than fixed automation. Model-free policies often struggle to close the reliability gap for VA tasks, which must be executed persistently and reliably in commercial and industrial applications. Motivated by prior work on Task and Motion Planning (TAMP) and the Robot Operating System (ROS), we introduce Graph-as-Policy (GaP), a multi-agent coding harness that generates directed computation graphs with perception, planning, and control nodes from a Modular Open Robot Skill Library (MORSL). GaP generates an internal simulation environment to rehearse task instances with different graphs in parallel to iteratively refine the graph structure and parameters to improve success rates and throughput. Evaluation with 8 new open VA task benchmarks, 4 in simulation and 4 in real-

10th Conference on Robot Learning (CoRL 2026), Austin TX, USA.

world, suggests that GaP can achieve success rates that significantly outperform baselines. Details, code, and data: https://graph-robots.github.io/gap

Keywords: Agentic Coding, Automation, Self-Learning

1 Introduction

A majority of robot learning research focuses on generalist robotics, where a robot must perform a broad variety of tasks. Most of this research has focused on model-free end-to-end Vision-Language-Action (VLA) models [7, 8, 9, 10, 11, 12]. However, fully generalist robots struggle to achieve commercial / industrial levels of reliability [13] and there is increasing interest in how robot learning could be useful for more specialized task classes [14]. In this paper, we identify a class of "Variational Automation (VA)" tasks that differ from "fixed automation" (which blindly repeats the same motions, e.g., spot welding or spray painting). In VA tasks, a robot persistently performs varying instances of a task with non-trivial variation in the geometry and pose of objects (e.g., to sort packages, make coffee in a cafe, or build sandwiches in a commercial kitchen). Today, fixed automation in logistics, service, agriculture, and manufacturing [15, 16, 17, 18] is set up and tuned by humans using rigorous, classical engineering methods. This provides high reliability and throughput, and human effort can be justified when amortized over years of repetitive performance. However, even more human effort is required to set up and tune VA systems for reliable performance.

Recent advances in Large Language Models (LLM) [19, 20, 21] and Vision-Language Models (VLM) [22, 23, 24, 25, 26] are rapidly improving agentic coding [27], semantic reasoning [28] and zero-shot generalization [29]. Agentic coding for robotics has the potential to integrate model-based and model-free paradigms to rapidly generate interpretable and reliable robot control systems. Agentic coding is new and advancing rapidly, but remains prone to hallucinations and constraint violations. Thus, a primary challenge is to develop effective methods for "steering" coding agents to produce desired outputs. Coding agents are controlled with a "harness" – a body of text provided as a prompt to the agents that describe available software resources, constraints, and performance metrics [30]. The harness also provides interfaces that allow the LLM to compile, execute, and manage generate-execute-observe-evaluate loops.

The use of LLM coding agents for robotics was explored as early as 2022 with a series of papers on Code-as-Policy (CaP) [31, 32]. General coding agents have improved dramatically since then by training on increasingly large coding datasets. The recent CaP-X paper provides an open suite of CaP benchmarks, agents, and encouraging results using coding agents that were state-of-the-art as of January 2026 [33]. These single-agent CaP approaches are somewhat unstructured, prompting the coding agent to generate free-form python code. For more complex tasks, the context window can grow sufficiently large so that it is difficult for the agent to obey constraints and converge on reliable code. Individual agents are also prone to hallucinations and "cheating", where they make up nonexistent skills or create trivial success metrics to artificially "solve" robot coding tasks. These challenges are exacerbated with *multi-agent* coding systems, where multiple agents operate in parallel.

To address these issues, we propose Graph-as-Policy (GaP), a harness structure that encapsulates modular robot functions into independent "nodes" in a directed graph that can be managed by a hierarchical multi-agent system where optimizing each node can be assigned to a specific agent. This structure also helps limit the size of each agent's context window and separates the graph generation from the graph testing to reduce incentives for individual coding agents to "cheat" in order to achieve requested objectives. GaP is inspired in part by the architecture of robot Task and Motion Planning (TAMP) systems [34, 35, 36] which use graphical hierarchies to ensure safety and the Robot Operating System (ROS)[3] which is based on a computation graph structure. Graphical models support modularity, reuse, and composability of functions in non-robotic and robotic applications. In GaP, a robot policy is a computation graph composed of atomic "skill" nodes, such as retrieving a camera frame, running inference on a perception model, or planning and executing a motion trajectory.

Given a VA task description, GaP starts with an Orchestration Agent that partitions a VA task into functional segments and instructs appropriate Skill Agents to synthesize localized, functional subgraphs of atomic nodes for its assigned segment. The orchestrator then aggregates and wires these subgraphs together into an executable computation graph. GaP then initiates a multi-agent self-learning harness that coordinates LLM and VLM agents to autonomously generate, simulate, evaluate, robot computation graphs in a loop with sampled task instances to increase a weighted combination of success rate and throughput until the combination reaches a plateau. The resulting computation graph is then sent to an edge-based graph interpreter for repeated execution on the robot.

To evaluate GaP, we present 8 new open VA benchmarks. The first 6 – based loosely on persistent commercial applications – are (I-a,b) Fulfill Grocery Orders, (II-a,b) Pack Grocery Items, and (III-a,b) Make Popcorn, where 'a' is in sim and 'b' is in real. These 6 ongoing tasks use common kitchen items and one Franka robot arm from the LIBERO [37] benchmark. The other two VA benchmarks – based loosely on datacenter and industrial applications – are (IV) Insert USB-C Cables, and (V) Wash Crates. Results suggest that GaP can achieve success rates that significantly outperform baselines, including $\pi_{0.5}$ [11] and MolmoAct2 [10].

This paper makes the following contributions: (1) the VA task class for robot learning with 8 open VA benchmarks; (2) a computation graph structure for agentic robotics; (3) GaP, an implemented multi-agent harness that autonomously decomposes natural language specifications to collaboratively generate robot computation graphs; (4) an open, evolving Modular Open Robot Skill Library (MORSL) with 51 initial skills; (5) a self-learning approach to graph rehearsal and optimization using the Newton physics simulator [6]; and (6) Experimental data comparing GaP with TAMP, model-free, and other baselines and simulations on the first 6 VA benchmarks, and performance results from GaP on the other 2 VA benchmarks.

2 Related Work

Variational Automation. The term "automation" is commonly used to describe robot systems that persistently perform repetitive tasks over hours, weeks, months, or years for logistics, manufacturing, healthcare, service, agriculture, and other applications. To be successful, commercial and industrial automation must achieve desired throughput (units per hour: success rate divided by cycle time) at a cost that will provide a desired return on investment. Accordingly, research in automation extends research in robotics by focusing on reliability, cost, safety, ease of use, and other factors required for successful production deployment.

In this paper, we propose "Variational Automation (VA)" as a class of tasks that differ from Generalist Robotics (GR) and Fixed Automation (FA). In FA, a robot persistently performs identical instances of a task. In box stacking, for example, FA would involve moving identical boxes from a common initial pose on a conveyor belt into a fixed pallet arrangement. In VA, a robot persistently performs varying instances of the task: the boxes have variable geometry (different SKUs), arrive in a distribution of varying initial poses, and must be densely packed into varying pallet arrangements. As most robot learning research focuses on GR, and robot learning may not be required for FA, we focus on robot learning for VA, aiming to reduce the human effort required to set up VA systems.

Modular Robot Control Methods. Early robotic systems programmed policies using classical modular components. The Shakey robot [38] in the late 1960s decomposed its architecture into 3 functional components: sensing, planning, and execution [39]. System architectures like the Robot Operating System (ROS) [3] utilize explicit directed graphs to route data, manage dependencies, and ensure reliable execution. Concurrently, Task and Motion Planning (TAMP) [34, 35] approaches jointly solve discrete task planning and continuous motion planning problems, enabling the satisfaction of constraints involving both high-level action sequencing and low-level geometric feasibility. Behavior Trees (BTs) [40] encode reactive task logic and failure recovery, and recent work shows LLMs can generate BTs with high success rates [41]. GaP combines the typed dataflow topology of the ROS computation graph with the reactive task logic and failure recovery of BTs, enabling (a) static type checking and verification, (b) explicit failure recovery loops, and (c) simulation-guided graph optimization.

Code-As-Policy for Robot Control. Code-as-Policy (CaP) uses agents to write robot control code, suggesting an alternative to manual coding of model-based methods and pure end-to-end learning of model-free policies [31]. Extensions such as ALGARA [42], CaP-X [33], CodeDiffuser [43], GRAPPA [44], and Maestro [45] use more recent LLMs to generate robot code. Similarly, systems like TiPToP [36] incorporate LLMs with classical robot TAMP [46, 47, 48, 49]; TAMP can achieve general open-vocabulary manipulation and transfer to new tasks with minimal tuning, and TiPToP integrates Gemini perception, M2T2 grasp planning, and cuTAMP. GaP explores an alternative modular architecture that specializes a persistent graph to a VA task class. GaP tempers the flexibility of CaP approaches by introducing a graph structure, allowing GaP to harness the open-world adaptivity of pretrained LLM coding agents while maintaining a structured, interpretable graph structure to support persistent Variational Automation.

3 Problem Formulation

Assumptions For Variational Automation tasks that will be repeated over extended periods, we assume the workcell environment, robot, and sensors are known and fixed. Furthermore, we assume the range of potential objects and the range of initial object poses are known. These assumptions are part of the VA setting rather than oracle information: unlike generalist robotics, VA tasks are defined by a known workcell and bounded operating envelope, allowing systems to use object models, calibrated sensors, and reusable automation skills when available. Because object meshes and pose ranges are part of the task input, the internal simulation is instantiated directly from them without scene reconstruction, system identification, or domain randomization.

Variational Automation Task Class We formalize a Variational Automation (VA) Task using the tuple $\mathcal{T} = \langle \mathcal{L}, \mathcal{E}, \mathcal{R}, \mathcal{O}, \mathcal{X}, \mathcal{B}, \mathcal{J} \rangle$:

- $\mathcal{L}$, Language Space: Natural language instructions and semantic descriptors that describe desired task behavior, providing high-level context for decomposing the task into segments.
- $\mathcal{E}$ is a known stationary workspace environment (e.g., workcell) that establishes world frame $\mathcal{W}$ and occupancy map $\mathcal{M}_E$, providing the support surfaces that constrain the feasible pose space of all entities to the non-colliding subset of $SE(3)$.
- $\mathcal{R}$ is the robot and sensor configuration, specifying the robot URDF, joint limits, gripper configuration, camera spec, and camera placement.
- $\mathcal{O}$, Object Set: The set of all possible objects in the task, comprising both rigid objects $\{o_i\}$ with 3D models $\mathcal{M}_i$ and articulated entities $\{\kappa_j\}$ (e.g., drawers, knobs) with defined kinematic joint limits $[\theta_{\min}, \theta_{\max}]$.
- $\mathcal{X}$, State Space: The product space of the robot joint configurations, the $SE(3)$ poses of all rigid objects, and the kinematic states of articulated entities: $\mathcal{X} = \mathcal{C}_{robot} \times SE(3)^n \times \mathbb{R}^m$.
- $\mathcal{B}$, Belief Space: Describes the distribution of objects and poses in instances of the task. A specific instance is sampled $\mathbf{x}_i \sim p(\mathbf{x} \mid \mathcal{X})$, introducing variations such as: (i) *Structured Priors:* Position sampled uniformly over a volume $\mathcal{V}$ ($\mathbf{x}_i \sim \text{Uniform}(\mathcal{V})$) and orientation ranges, and (ii) *Empirical Distributions:* Multi-modal distributions estimated from real-world demonstrations or perception (e.g., point cloud registration).
- $\mathcal{J}$, Reward function: A multi-objective reward function used to evaluate success and efficiency, defined as: $\mathcal{J} = w_s \cdot \mathbb{I}(\text{success}) + w_t \cdot \Phi$ where $\mathbb{I}(\cdot)$ is the success indicator, Φ is the throughput (success rate / cycle time), and w_s, w_t are weighting factors.

Given a task $\mathcal{T}$, a task instance $\tau_i = \langle o_i, x_i \rangle$ is drawn from $\mathcal{O}$ and $\mathcal{B}$ respectively. **Policy Representation via Directed Execution Graphs** Graph-as-policy (GaP) represents a robot policy $\pi(a \mid \mathbf{x}, \mathcal{T})$ as a directed computation graph $\mathcal{G} = (V, E)$ to complete all task instances $\forall \tau_i \in \mathcal{T}$. The graph $\mathcal{G}$ consists of modular, atomic functional units called *nodes*, connected by edges that dictate both data flow and execution logic. Nodes can be grouped into *skills*, a natural-language specification that instructs an LLM agent how to configure and compose a set of atomic nodes on the execution graph for a defined sub-task.

Problem Definition Given a task class $\mathcal{T} = \langle \mathcal{L}, \mathcal{E}, \mathcal{R}, \mathcal{O}, \mathcal{X}, \mathcal{B}, \mathcal{J} \rangle$, GaP must synthesize a robust execution graph $\mathcal{G}^*$ that generalizes across the entire belief space $\mathcal{B}$. Formally, for any task instance $\tau_i \in \mathcal{T}$ and given a real-time scene observation $\mathcal{I}$ (comprising multi-view image sets from static and

wrist cameras), the graph executor interprets the computation graph $\mathcal{G}^*$ by invoking its skill nodes and following its data and control edges. This execution induces a closed-loop robot policy $\pi_G(a \mid \mathcal{I})$, which maps observations and graph state to robot actions in order to achieve the goal state specified by $\mathcal{L}$. We define the optimized graph $\mathcal{G}^*$ as one that maximizes performance across all instances in the variational class: $\mathcal{G}^* = \arg\max_{\mathcal{G}} \mathbb{E}_{x_i \sim \mathcal{B}} [\mathcal{J}(\pi(a \mid \mathcal{I}, \mathcal{G}))]$. The optimized graph is then sent to an edge-based interpreter for repeated execution on the robot.

4 Graph-as-Policy

The GaP architecture is illustrated in Figure 1. As an example, consider the Make Popcorn VA task. Given a natural language specification and geometric object models, the multi-agent GaP harness first partitions the high-level objective into semantic segments such as 'turn on the knob', 'pick up the popcorn pan', etc. Next, drawing from the Modular Open Robot Skill Library (MORSL), GaP maps these segments into atomic robotic skills to synthesize an initial computation graph $\mathcal{G}$. During self-learning, the computation graph is evaluated using an internal simulation to iteratively refine the execution graph topology and node parameters prior to deployment. The optimized robot computation graph is then sent to an external interpreter for repeated execution on the physical robot.

4.1 Modular Open Robot Skill Library (MORSL)

The MORSL library uses agentic tool-use conventions (e.g., Anthropic's `Skill.md` [50]) with extensions for graph declarations. Each skill declares its inputs, outputs, semantic parameters, and pre-conditions, so the agent can decide both when to invoke it and how to wire it into the graph. Examples of the 51 initial MORSL skills include perception, grasp planning, motion planning, 2D/3D vision utilities, and verification and control primitives [51, 52, 53, 54, 55, 24, 56, 57, 4, 58, 59, 60], including (*) Cartesian Linear Motion Planning with CuRobo; (*) Robot Operating System (ROS) Translator ; (*) Visuomotor Interactive Perception Policies.

4.2 Self-Learning through Internal Simulation Rehearsal

To iteratively learn to improve a graph using task instances, we execute the computation graph, provide feedback, update the graph, and iterate. GaP uses Newton simulator [6] as an internal simulation to render the visualization for the perception nodes, simulate physics, and compute contacts. To generate feedback, GaP registers the robot and object state before and after each rehearsing node, together with contact queries between the robot and objects, to compute differences and infer the motion outcome. The optimization process begins with task instance sampling, where the system generates N parallel task instances $\{\tau_i\}_{i=1}^{N}$. These task instances are instantiated by sampling from the belief space $\mathcal{B}$, which represents the probability distribution over potential object poses, initial states, and kinematic configurations within the workspace $\mathcal{E}$. GaP generates the initial graph $\mathcal{G}_0$ through multi-agent harness. Then, a parallel rehearsal starts across these N scenes to evaluate graph performance. In instances where the rollout fails to meet success criteria, GaP analyzes the physical execution data to isolate geometric root causes within the occupancy or articulated entities. The graph is updated by the agents with Graph Update using a typed action set: (1) set a node's declared inputs, such as perception prompts; (2) rewire node inputs and outputs; (3) rewrite an inline Python script, such as format transformations and arithmetic; (4) swap skill nodes; and (5) implement a node. Proposed updates that degrade success rate or cycle time on 100 fresh task instances are rejected, and the loop iterates until performance reaches a plateau or terminates with failure reasons.

5 Experiments

5.1 Simulation and Real-World Variational Automation Benchmarks

We present 8 VA benchmark tasks, including 4 in simulation and 4 in real-world. Six of these are inspired by LIBERO [37], the de facto standard for evaluating VLA policies in simulation. **Benchmark (I-a,b): Fulfill Grocery Orders (Sim and Real)** Each instance of this task involves locating a designated target item and placing it into the basket. The original LIBERO [37] benchmark did not vary the position of the (*objects*) which allows for overfitting to the demonstration examples. To address this, the LIBERO-Pro [61] evaluation suite swaps target and basket object positions at

test time (*object_swap*). We introduce four extensions for our VA Benchmarks: 1) *X-Y 20×20 cm^2*, where the position of each object varies uniformly within a 20×20 cm^2 zone centered around the original LIBERO object pose; 2) *basket_swap*, which swaps the target item and basket location; 3) *permutation*, which swaps target item and distractor item positions; and *mixed_all* including all three variation types. The physical benchmark directly mirrors this setup. To avoid object collisions during task instance generation, we utilize Minkowski sum [62] operations to ensure item singulation. The real version of this benchmarks uses a Franka arm with wrist camera and real items from a grocery store. **Benchmark (II-a,b): Pack Grocery Items (Sim and Real)** We modify Benchmark I-a,b to create multi-object pick-and-place tasks, as in a grocery checkout line, where the robot is assigned to pack 6 objects into a container without needing to identify or select any specific items. We quantify the success rate as the number of items (out of 6) placed into the basket after 6 grasping attempts. **Benchmark (III-a,b): Make Popcorn (Sim and Real)** We use the LIBERO frypan, stove, and knob assets to create a manipulation task that requires the robot to sequentially turn on a stove, pick up the pan handle, place it on the stove, remove the pan, and turn off the stove. For the real version of this benchmark, we use the Franka Robot arm with wrist-camera, a portable stove from Amazon and Jiffy-Pop popcorn. **Benchmark (IV): Insert USB-C Cables (Real)** This benchmark task requires a UR5 robot arm with the ZED Mini wrist camera to execute a series of USB-C cable insertions and extractions in a bank of 7 sockets. The robot uses internal force torque feedback to probe the insertion when the target port goes beyond the camera's field of view. The benchmark includes two varying conditions. First, we vary the pose of the cable ports, testing three distances in 5 cm increments and three angles in 15° increments. Second, we vary the text prompt to specify five distinct goals: targeting individual ports, inserting in ascending order, descending order, odd-indexed ports, and even-indexed ports. **Benchmark (V): Wash Crates (Sim)** This simulation benchmark simulates a real industrial crate-washing use case where two Franka robot arms must cooperatively grasp a crate by narrow slits on its sides, lift it off a stack, flip it, and place it onto a washing machine table. Each instance varies the initial pose of the crate, varying yaw rotations of up to $\pm 15°$ and horizontal displacements of up to ± 2.5 cm. Each benchmark provides a language instruction.

5.2 Baselines

Each cell in Table 1 represents the outcome from trials with 100 task instances of Benchmarks I-a and II-a (in simulation) for a total of over 5000 simulation trials. We run CaP-X [33] which uses a single agent and is given only an image of the initial task instance and natural language instructions. We note that this is not a fair comparison as GaP is designed for Variational Automation where environment geometry is known (but object location is unknown), so the performance of CaP-X serves as an ablation of GaP with a single agent and without self-learning. We evaluate VLA models $\pi_{0.5}$ [11] and MolmoAct2 [10] with official checkpoints finetuned on the LIBERO training dataset. We also evaluate TipTop [36], a modular open-vocabulary planning system for robotic manipulation based on TAMP. We configure this from the github code with the default configuration of 128 particles for cuTAMP [63] with a 60-second planning timeout. We warm up the cuTAMP cache before measuring the execution time. Rows 5 and 6 represent combinations of GaP with VLA models, where GaP generates an initial robot motion to center the wrist camera over the target object (bringing the VLA into distribution). For GaP and CaP-X, we use Gemini-3.1-Flash-Lite for LLM agents and VLM with a temperature of 0.1. For Benchmarks I and II, GaP does not perform self-learning because the first graph generated achieves high performance.

5.3 Benchmarks I and II: Fulfill Grocery Orders and Pack Grocery Items

5.3.1 Simulation Results

GaP achieves significantly better positional robustness compared to baselines. As shown in Table 1, while baseline VLA models ($\pi_{0.5}$, MolmoAct2) achieve high success rates on LIBERO-object without pose variation, their performance drops as low as 0.20 for LIBERO-PRO with positional variance. In contrast, GaP maintains robust success rates across all variations. We find

Table 1: **Success Rates for 5500 trials, 100 task instances per table cell. Results on Benchmarks I-a and II-a: Fulfill Grocery Orders and Pack Grocery Items**. The first two columns are the original LIBERO [37] with negligible pose variation, and LIBERO-PRO with slightly larger pose variation [61] . We introduce the VA Grocery Order Fulfillment benchmark that includes larger object positional variance (X-Y 20×20 cm^2), swapping target and basket positions (basket_swap), permuting all item locations, and everything combined (mixed_all). We also introduce the Grocery Packing benchmark that requires picking all objects and placing them in the basket. In rows 5 and 6, GaP navigates the robot wrist camera above the target object and then switches to MolmoAct2 and $\pi_{0.5}$ VLA policies.

	LIBERO	LIBERO-Pro	Fulfill Grocery Orders				Pack Grocery Items	
Method	object	object_swap	X-Y 20×20 cm^2	basket_swap	permutation	mixed_all	fixed	varied
CaP-X	-	0.22	0.07	0.05	0.11	0.10	0.01	0.01
$\pi_{0.5}$	0.96	0.24	0.78	0.15	0.20	0.20	0.17	0.18
MolmoAct2	**0.97**	0.43	0.90	0.26	0.10	0.20	0.18	0.18
TipTop	0.22	0.22	0.29	0.24	0.31	0.24	0.34	0.46
$\pi_{0.5}$ w/GaP	0.85	0.60	0.79	0.32	0.50	0.39	0.67	0.66
MolmoAct2 w/GaP	0.70	0.62	0.84	0.58	0.39	0.66	0.59	0.59
GaP	0.95	**0.95**	**0.95**	**0.97**	**0.93**	**0.97**	**0.99**	**0.98**

that TipTop [36] cannot generate motion plans for many of these benchmark task instances because M2T2 [58], cuRobo [59], and cuTAMP [63] cannot plan feasible solutions.

VLA policies can benefit from GaP. Performance for $\pi_{0.5}$ w/GaP and MolmoAct2 w/GaP suggest that GaP can enhance robustness of existing VLA models as shown in rows 5 and 6 of Table 1. As VLA policies struggle with positional perturbation of target objects, GaP uses the wrist camera and interactive perception skills to reliably identify the target object and uses linear cartesian motion skills to navigate the arm and wrist camera to a pre-grasp pose above the target object. The GaP computation graph then hands over execution to the VLA policy, staging it from a more favorable observation and producing more than a twofold improvement in success rates.

5.3.2 Real Physical Experiment Results

GaP transfers well from Sim to Real. Table 2 For the Fulfill Grocery Orders benchmark, GaP achieves a perfect success rate of 25/25 (100%), while TipTop succeeds in only 8/25 trials. Both GaP and TipTop accurately identify the objects. However, TipTop [36] fails because M2T2 [58], cuRobo [59], and cuTAMP [63] combined cannot find feasible motion plans for cubic-shaped objects, tall baskets, or varied object orientations. In terms of execution time, GaP perceives the item and basket in parallel using 14.1 seconds to generate oriented bounding boxes, and 36.4 seconds for descending, grasping, and transporting the items.

Table 2: **Physical Benchmark on Benchmark I-b , Benchmark II-b and Benchmark III-b** . We report success rate and completion time. Sub-tasks (→) are reported per benchmark. On average, the completion time of single pick-and-place for TipTop is 95 seconds, and GaP is 67 seconds.

Success Rate	TipTop	GaP
Fulfill Grocery Orders	8/25	**25/25**
→ object	3/5	5/5
→ 20x20	2/5	5/5
→ basket swap	1/5	5/5
→ tall basket	0/5	5/5
→ permutation	2/5	5/5
Pack Grocery Items	10/30	**28/30**
Make Popcorn	0/20	**18/20**

5.4 Ablation Studies

For Fulfilling Grocery Orders and Packing Grocery Items, the full GaP system achieves robust success rates (0.93–0.99). We ablate as follows: (1) **Graphless generation** forces the LLM to perfectly inline low-level service interfaces, such as method names and request schemas, from memory. Consequently, even when the high-level logic is correct, minor syntax or interface mismatch errors inevitably terminate the trial. So replacing the structured graph output with a single LLM that generates raw Python scripts collapses the success rate to zero. (2) **Condensing GaP's specialized authoring agents into a single LLM** also drops success rates to zero, with all trials failing static structural verification prior to execution, because a single LLM agent struggles to simultaneously manage global data flow, local logic, and verification, frequently introducing dangling references or node collisions. Furthermore, even with iterative feedback, a single LLM tends to oscillate between mistake classes without converging. (3) **Graph validation improves performance**. For each configuration in Fulfill Grocery Orders, some task segmentation agents emit a first-attempt subgraph that fails static type/edge checks and would crash at runtime, for example, some graphs wire the input and output of the transport phase in drop-pose computation to the release phase and

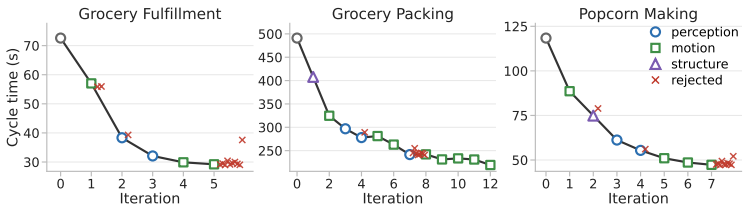


Figure 3: **Self-Learning to reduce Cycle Time on Benchmarks I–III.** Per-iteration cycle time (left axis) and success rate (right axis). Accepted graph updates are colored by edit class: perception (blue), motion parameters (green), and graph topology (purple); updates that degrade success rate or cycle time on 100 fresh task instances are rejected.

Table 3: **Success rate and throughput before and after self-learning on Benchmarks I–III (simulation).** TiPToP w/ MORSL replaces TiPToP's perception and grasp planning with MORSL skills.

	Success Rate ↑				Throughput (cycles/hr) ↑	
Benchmark	**TiPToP**	**TiPToP w/ MORSL**	**GaP (Initial)**	**GaP (Learned)**	**GaP (Initial)**	**GaP (Learned)**
I. Fulfill Grocery Orders	0.24	0.53	**0.97**	**0.97**	49.7	**124.1**
II. Pack Grocery Items	0.34	0.60	**0.97**	**0.97**	7.3	**16.2**
III. Make Popcorn	0.00	0.00	0.33	**0.94**	30.5	**76.6**

other is in checkpoint verification. GaP's graph validation verifies the wiring and effectively ensures the graph edge connectivity.

5.5 Self-Learning Can Increase Success Rate

The Make Popcorn task requires the robot to grasps the stove knob and rotate it to turn on the burner, then the robot must find and pick up the handle of the JiffyPop popcorn pan, place it on the stove burner, wait, and then turn off the stove. GaP generates a graph using GraspGen [4], knob turning skills and other object localization and grasping skills from Benchmark 1 and 2. The initial graph is able to turn on and off the knob but unable to pick and place the pan properly with only a 33% success rate.

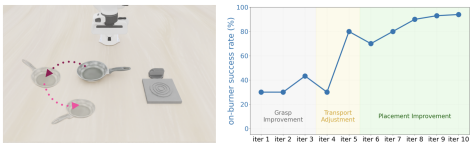


Figure 2: **Self-Learning for Making Popcorn Benchmark.** Pan pose variations (left) drive a 10-iteration sequence of graph updates; (blue, left axis) iteration phases shaded by class of edit.

As shown in the Fig. 2, self-learning proceeds through three stages: (1) from iteration 1 to 3, the majority of failures come from pan grasping failure, where the simulator feedback reports that the Franka gripper is not in contact with the object pan, so GaP replaces the GraspGen grasp skill with a skill that mixes GraspGen with an oriented bounding box grasp planner. (2) In iteration 4, GaP recognizes that the pan should be grasped by the handle, thereby adjusting the perception algorithm prompts to localize the pan handle. (3) In iterations 4-8, GaP finetunes the offset of pan placement due to the changed grasping strategy to align the pan with the stove surface. The resulting policy achieves 94% in simulation with variations in pan position and orientation, and achieves a 90% (18/20) success rate in real physical trials as shown in Table 2. The two physical failures resulted from one inverse kinematics (IK) error during linear Cartesian motion, and one misgrasp caused by accumulated kinematic error.

5.6 Self-Learning Can Reduce Cycle Time

Since GaP saturates the success rate on Benchmarks I–III, we additionally run self-learning with the throughput term of $\mathcal{J}$ to reduce cycle time. As shown in Fig. 3 and Table 3, the LLM agent reduces cycle time by up to **57%** with no success rate trade-off. It adjusts perception algorithms (e.g., using a faster detector for the basket), tunes motion parameters (e.g., control settling steps), and modifies graph topology (e.g., reusing perception results across nodes); proposals that degrade success rate or cycle time on 100 fresh task instances are rejected by the internal simulation. Table 3 also reports TiPToP equipped with MORSL perception and grasp planning skills: TAMP benefits from the higher-quality MORSL skills, while GaP further improves performance with flexible motion primitives and self-learning. In terms of practical cost, graph generation takes fewer than 30 LLM

calls to Gemini (about $0.01 and 1 s latency); self-learning wall-clock time is dominated by simulation (about 15 minutes per iteration and up to 150 minutes in total for Make Popcorn); and no agent is needed once the graph is deployed.

5.7 Benchmark IV: Insert USB-C Cables (Real)

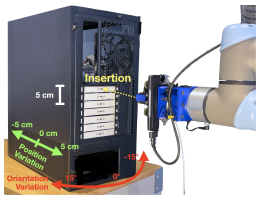


Figure 4: Benchmark IV: Seven-ports cable insertion setup.

Table 4: **Benchmark IV USB-C Cable insertion results over 130 total instances**. Success rates (SR) and execution time in seconds (ET).

Variation	SR (Per trial)	SR (All)	ET (All)
Insertion Goal Condition			
Individual port*	5/5	-	26.0
Ascending order	32/35	2/5	247.0
Descending order	32/35	4/5	223.2
Odd index port	20/20	5/5	136.8
Even index port	14/15	4/5	104.6
Position/Orientation			
-15°*	4/5	-	24.0
15°*	5/5	-	25.6
-5 cm*	5/5	-	29.4
5 cm*	4/5	-	28.0

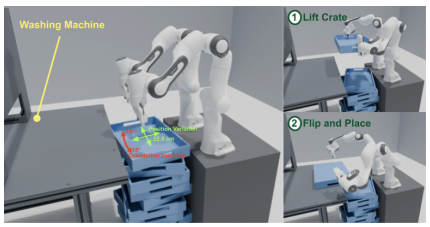


Figure 5: Industrial crate-washing setup.

For cable insertion benchmark evaluation, we utilize the computation graph generated by GaP, which operates via four modular ROS execution nodes: *align to port*, *touch port*, *insert*, *extract*. The robot first aligns to establish contact, generating a $1 \times 1\ cm^2$ grid of insertion candidates. The *insert* node then evaluates these positions, requiring $>$3 mm of progress at $<$10.0 N of force, and confirms successful insertion when the depth exceeds 6 mm at 30.0 N. Finally, the *extract* node safely pulls the cable using a 2.0 Hz wiggling motion while maintaining lateral forces below 20.0 N. This entire policy requires approximately 30 seconds per insertion. We discuss the result in the Appendix.

5.8 Benchmark V: Wash Crates (Simulation)

We compare GaP with a hand-engineered execution graph authored by an expert, representing the conventional manual engineering effort required in such settings. We run both policies over 150 trials sampled from the pose distribution, and additionally measure sustained throughput over a 3-hour continuous execution window.

GaP closely matches an expert hand-engineered solution. GaP achieves a $0.953\ (143/150)$ success rate against the hand-engineered graph's $0.987\ (148/150)$, with similar average cycle times (179.13 s vs. 176.47 s). Over the 3-hour throughput run both policies attempted 59 trials, of which GaP completed 55 and the hand-engineered graph 58, corresponding to 18.33 and 19.33 successes per hour, respectively. These results suggest that GaP can autonomously produce coordinated bimanual policies whose reliability and throughput approach those of a manually hand-tuned baseline.

6 Conclusion

Agentic robotics has potential to build on rapidly-advancing LLM models to provide a bridge between Good Old Fashioned Engineering (GOFE) and model-free VLA policies. GaP's graph-structured agentic robotics facilitates modularity, multi-agent integration, and self-learning. As robot applications become more complex and skill libraries grow, more sophisticated agent harnessing will be required.

Limitations. Although in experiments, GaP improves success rates significantly over baselines, execution reliability is not yet at industry levels and additional self-learning and parameter tuning is required. Similarly, GaP execution times are still well below industry standards of 500 units per hour (7 seconds per instance); more work is required to reduce VLM inference requests and IK motion planning time during execution. Also, the 8 VA benchmarks focus on quasi-static pick-and-place operations – only Cable Insertion (IV) requires force sensing. More work is required to apply GaP to tasks with deformable objects, dynamic forces, and moving targets.

References

[1] Anthropic. Claude 3.5 Sonnet. https://www.anthropic.com/news/claude-3-5-sonnet, June 2024.

[2] K. Kavukcuoglu. Gemini 2.5: Our most intelligent AI model. https://blog.google/technology/google-deepmind/gemini-model-thinking-updates-march-2025/, Mar. 2025.

[3] S. Macenski, T. Foote, B. Gerkey, C. Lalancette, and W. Woodall. Robot operating system 2: Design, architecture, and uses in the wild. *Science robotics*, 7(66):eabm6074, 2022.

[4] A. Murali, B. Sundaralingam, Y.-W. Chao, J. Yamada, W. Yuan, M. Carlson, F. Ramos, S. Birchfield, D. Fox, and C. Eppner. Graspgen: A diffusion-based framework for 6-dof grasping with on-generator training. In *Proceedings of the IEEE International Conference on Robotics and Automation (ICRA)*. IEEE, 2026.

[5] NVIDIA. Isaac Sim. URL https://github.com/isaac-sim/IsaacSim.

[6] The Newton Contributors. Newton: GPU-accelerated physics simulation for robotics and simulation research, Apr. 2025. URL https://github.com/newton-physics/newton.

[7] M. Kim, K. Pertsch, S. Karamcheti, T. Xiao, A. Balakrishna, S. Nair, R. Rafailov, E. Foster, G. Lam, P. Sanketi, Q. Vuong, T. Kollar, B. Burchfiel, R. Tedrake, D. Sadigh, S. Levine, P. Liang, and C. Finn. Openvla: An open-source vision-language-action model. *arXiv preprint arXiv:2406.09246*, 2024.

[8] P. I. Team. π_0: A vision-language-action flow model for general robot control. *arXiv preprint arXiv:2410.24164*, 2024.

[9] O. X.-E. Co-Authors. Open X-Embodiment: Robotic learning datasets and RT-X models. In *2024 IEEE International Conference on Robotics and Automation (ICRA)*, pages 6892–6903. IEEE, 2024.

[10] H. Fang, J. Duan, D. Clay, S. Wang, S. Liu, W. Huang, X. Fan, W.-C. Tsai, S. Chen, Y. R. Wang, et al. Molmoact2: Action reasoning models for real-world deployment. *arXiv preprint arXiv:2605.02881*, 2026.

[11] K. Black, N. Brown, J. Darpinian, K. Dhabalia, D. Driess, A. Esmail, M. R. Equi, C. Finn, N. Fusai, M. Y. Galliker, et al. $\pi_{0.5}$: a vision-language-action model with open-world generalization. In *9th Annual Conference on Robot Learning*, 2025.

[12] M. Zawalski, W. Chen, K. Pertsch, O. Mees, C. Finn, and S. Levine. Robotic control via embodied chain-of-thought reasoning. In *Conference on Robot Learning*, pages 3157–3181. PMLR, 2025.

[13] J. Gao, S. Belkhale, S. Dasari, A. Balakrishna, D. Shah, and D. Sadigh. A taxonomy for evaluating generalist robot manipulation policies. *IEEE Robotics and Automation Letters (RA-L)*, 2026.

[14] K. Goldberg. Should robot generalists get off their high horse?, 2026. Available online.

[15] E. Solowjow, I. Ugalde, Y. Shahapurkar, J. Aparicio, J. Mahler, V. Satish, K. Goldberg, and H. Claussen. Industrial robot grasping with deep learning using a programmable logic controller (plc). In *2020 IEEE 16th International Conference on Automation Science and Engineering (CASE)*, pages 97–103, 2020. doi:10.1109/CASE48305.2020.9216902.

[16] S. Adebola, T. Sadjadpour, K. El-Refai, W. Panitch, Z. Ma, R. Lin, T. Qiu, S. Ganti, C. Le, J. Drake, and K. Goldberg. Automating deformable gasket assembly. In *2024 IEEE 20th International Conference on Automation Science and Engineering (CASE)*, pages 4146–4153. IEEE, 2024.

[17] S. Xie, K. Goldberg, and D. Song. Energy efficient planning for repetitive heterogeneous tasks in precision agriculture. In *2025 IEEE International Conference on Robotics and Automation (ICRA)*, pages 7139–7145, 2025. doi:10.1109/ICRA55743.2025.11128083.

[18] S. Adebola, R. Parikh, M. Presten, S. Sharma, S. Aeron, A. Rao, S. Mukherjee, T. Qu, C. Wistrom, E. Solowjow, and K. Goldberg. Can machines garden? systematically comparing the alphagarden vs. professional horticulturalists. In *2023 IEEE International Conference on Robotics and Automation (ICRA)*, pages 11779–11785, 2023. doi:10.1109/ICRA48891.2023.10161497.

[19] Q. Team. Qwen3. 5-omni technical report. *arXiv preprint arXiv:2604.15804*, 2026.

[20] A. Yang, A. Li, B. Yang, B. Zhang, B. Hui, B. Zheng, B. Yu, C. Gao, C. Huang, C. Lv, et al. Qwen3 technical report. *arXiv preprint arXiv:2505.09388*, 2025.

[21] D. Guo, D. Yang, H. Zhang, J. Song, P. Wang, Q. Zhu, R. Xu, R. Zhang, S. Ma, X. Bi, et al. Deepseek-r1: Incentivizing reasoning capability in llms via reinforcement learning. *arXiv preprint arXiv:2501.12948*, 2025.

[22] A. Radford, J. W. Kim, C. Hallacy, A. Ramesh, G. Goh, S. Agarwal, G. Sastry, A. Askell, P. Mishkin, J. Clark, G. Krueger, and I. Sutskever. Learning transferable visual models from natural language supervision. In M. Meila and T. Zhang, editors, *Proceedings of the 38th International Conference on Machine Learning*, volume 139 of *Proceedings of Machine Learning Research*, pages 8748–8763. PMLR, 18–24 Jul 2021.

[23] F. Bordes, R. Y. Pang, A. Ajay, A. C. Li, A. Bardes, S. Petryk, O. Mañas, Z. Lin, A. Mahmoud, B. Jayaraman, et al. An introduction to vision-language modeling. *arXiv preprint arXiv:2405.17247*, 2024.

[24] G. R. Team, S. Abeyruwan, et al. Gemini robotics: Bringing ai into the physical world, 2025. URL https://arxiv.org/abs/2503.20020.

[25] W. Huang, C. Wang, R. Zhang, Y. Li, J. Wu, and L. Fei-Fei. Voxposer: Composable 3d value maps for robotic manipulation with language models. In *Conference on Robot Learning*, pages 540–562. PMLR, 2023.

[26] C. Ning, K. Fang, and W.-C. Ma. Prompting with the future: Open-world model predictive control with interactive digital twins. In *Proceedings of Robotics: Science and Systems (RSS)*, 2025.

[27] Anthropic. Claude 3.5 Sonnet. https://www.anthropic.com/product/claude-code, June 2024.

[28] K. Chen, S. Xie, Z. Ma, P. R. Sanketi, and K. Goldberg. Robo2vlm: Improving visual question answering using large-scale robot manipulation data. In *The Thirty-ninth Annual Conference on Neural Information Processing Systems Datasets and Benchmarks Track*, 2025.

[29] Y. Ji, H. Tan, J. Shi, X. Hao, Y. Zhang, H. Zhang, P. Wang, M. Zhao, Y. Mu, P. An, et al. Robobrain: A unified brain model for robotic manipulation from abstract to concrete. *CVPR*, 2025.

[30] Anthropic. Harness design for long-running application development. https://www.anthropic.com/engineering/harness-design-long-running-apps, Mar. 2026.

[31] J. Liang, W. Huang, F. Xia, P. Xu, K. Hausman, B. Ichter, P. Florence, and A. Zeng. Code as policies: Language model programs for embodied control. In *2023 IEEE International conference on robotics and automation (ICRA)*, pages 9493–9500. IEEE, 2023.

[32] G. Yin, Y. Li, Y. Wang, D. Mcconachie, P. Shah, K. Hashimoto, H. Zhang, K. Liu, and Y. Li. CodeDiffuser: Attention-Enhanced Diffusion Policy via VLM-Generated Code for Instruction Ambiguity. In *Proceedings of Robotics: Science and Systems*, LosAngeles, CA, USA, June 2025. doi:10.15607/RSS.2025.XXI.072.

[33] M. Fu, J. Yu, K. El-Refai, E. Kou, H. Xue, H. Huang, W. Xiao, G. Wang, F.-F. Li, G. Shi, et al. Cap-x: A framework for benchmarking and improving coding agents for robot manipulation. *arXiv preprint arXiv:2603.22435*, 2026.

[34] L. P. Kaelbling and T. Lozano-Pérez. Hierarchical task and motion planning in the now. In *2011 IEEE international conference on robotics and automation*, pages 1470–1477. IEEE, 2011.

[35] C. R. Garrett, R. Chitnis, R. Holladay, B. Kim, T. Silver, L. P. Kaelbling, and T. Lozano-Pérez. Integrated task and motion planning. *Annual review of control, robotics, and autonomous systems*, 4(1):265–293, 2021.

[36] W. Shen, N. Kumar, S. Chintalapudi, J. Wang, C. Watson, E. S. Hu, J. Cao, D. Jayaraman, L. P. Kaelbling, and T. Lozano-Pérez. TiPToP: A modular open-vocabulary planning system for robotic manipulation. *arXiv preprint arXiv:2603.09971*, 2026.

[37] B. Liu, Y. Zhu, C. Gao, Y. Feng, Q. Liu, Y. Zhu, and P. Stone. Libero: Benchmarking knowledge transfer for lifelong robot learning. *Advances in Neural Information Processing Systems*, 36: 44776–44791, 2023.

[38] N. J. Nilsson. *Artificial intelligence: a new synthesis*. Elsevier, 1998.

[39] N. J. Nilsson. *Principles of artificial intelligence*. Morgan Kaufmann, 2014.

[40] M. Colledanchise and P. Ögren. *Behavior Trees in Robotics and AI: An Introduction*. CRC Press, 2018.

[41] R. A. Izzo, G. Bardaro, and M. Matteucci. BTGenBot: Behavior tree generation for robotic tasks with lightweight LLMs. *arXiv preprint arXiv:2403.12761*, 2024.

[42] N. Cote, J. Drake, and S. Chitta. Agentic language-grounded adaptive robotic assembly. In *The first CVPR workshop on 3D Vision Language Models (VLMs) for Robotics Manipulation: Opportunities and Challenges*, 2024.

[43] G. Yin, Y. Li, Y. Wang, D. Mcconachie, P. Shah, K. Hashimoto, H. Zhang, K. Liu, and Y. Li. CodeDiffuser: Attention-Enhanced Diffusion Policy via VLM-Generated Code for Instruction Ambiguity. In *Proceedings of Robotics: Science and Systems*, LosAngeles, CA, USA, June 2025. doi:10.15607/RSS.2025.XXI.072.

[44] A. Bucker, P. Ortega-Kral, J. Francis, and J. Oh. Grappa: Generalizing and adapting robot policies via online agentic guidance. *IEEE Robotics and Automation Letters*, 2026.

[45] J. Shi, R. Yang, K. Chao, B. S. Wan, Y. S. Shao, J. Lei, J. Qian, L. Le, P. Chaudhari, K. Daniilidis, et al. Maestro: Orchestrating robotics modules with vision-language models for zero-shot generalist robots. In *NeurIPS 2025 Workshop on Space in Vision, Language, and Embodied AI*, 2025.

[46] S. Wang, M. Han, Z. Jiao, Z. Zhang, Y. N. Wu, S.-C. Zhu, and H. Liu. LLM3: Large Language Model-based Task and Motion Planning with Motion Failure Reasoning. In *2024 IEEE/RSJ international conference on intelligent robots and systems (IROS)*, pages 12086–12092. IEEE, 2024.

[47] A. Curtis, N. Kumar, J. Cao, T. Lozano-Pérez, and L. P. Kaelbling. Trust the proc3s: Solving long-horizon robotics problems with llms and constraint satisfaction. In *Conference on Robot Learning*, pages 1362–1383. PMLR, 2025.

[48] Z. Yang, C. Garrett, D. Fox, T. Lozano-Pérez, and L. P. Kaelbling. Guiding long-horizon task and motion planning with vision language models. In *2025 IEEE International Conference on Robotics and Automation (ICRA)*, pages 16847–16853. IEEE, 2025.

[49] N. Kumar, W. Shen, F. Ramos, D. Fox, T. Lozano-Pérez, L. P. Kaelbling, and C. R. Garrett. Open-world task and motion planning via vision-language model generated constraints. *IEEE Robotics and Automation Letters*, 2026.

[50] Anthropic. Equipping agents for the real world with Agent Skills. https://www.anthropic.com/engineering/equipping-agents-for-the-real-world-with-agent-skills, Oct. 2025.

[51] N. Ravi, V. Gabeur, Y.-T. Hu, R. Hu, C. Ryali, T. Ma, H. Khedr, R. Rädle, C. Rolland, L. Gustafson, et al. Sam 2: Segment anything in images and videos. In *International Conference on Learning Representations*, volume 2025, pages 28085–28128, 2025.

[52] N. Carion, L. Gustafson, Y.-T. Hu, S. Debnath, R. Hu, D. Suris, C. Ryali, K. V. Alwala, H. Khedr, A. Huang, J. Lei, T. Ma, B. Guo, A. Kalla, M. Marks, J. Greer, M. Wang, P. Sun, R. Rädle, T. Afouras, E. Mavroudi, K. Xu, T.-H. Wu, Y. Zhou, L. Momeni, R. Hazra, S. Ding, S. Vaze, F. Porcher, F. Li, S. Li, A. Kamath, H. K. Cheng, P. Dollár, N. Ravi, K. Saenko, P. Zhang, and C. Feichtenhofer. Sam 3: Segment anything with concepts, 2025. URL https://arxiv.org/abs/2511.16719.

[53] S. Liu, Z. Zeng, T. Ren, F. Li, H. Zhang, J. Yang, Q. Jiang, C. Li, J. Yang, H. Su, et al. Grounding dino: Marrying dino with grounded pre-training for open-set object detection. In *European Conference on Computer Vision*, pages 38–55. Springer, 2024.

[54] M. Minderer, A. Gritsenko, A. Stone, M. Neumann, D. Weissenborn, A. Dosovitskiy, A. Mahendran, A. Arnab, M. Dehghani, Z. Shen, et al. Simple open-vocabulary object detection. In *European conference on computer vision*, pages 728–755. Springer, 2022.

[55] M. Deitke, C. Clark, S. Lee, R. Tripathi, Y. Yang, J. S. Park, M. Salehi, N. Muennighoff, K. Lo, L. Soldaini, et al. Molmo and pixmo: Open weights and open data for state-of-the-art vision-language models. In *2025 IEEE/CVF Conference on Computer Vision and Pattern Recognition (CVPR)*, pages 91–104. IEEE, 2025.

[56] A. Kamath, J. Ferret, S. Pathak, N. Vieillard, R. Merhej, S. Perrin, T. Matejovicova, A. Ramé, M. Rivière, L. Rouillard, et al. Gemma 3 technical report. *arXiv preprint arXiv:2503.19786*, 4, 2025.

[57] M. Sundermeyer, A. Mousavian, R. Triebel, and D. Fox. Contact-graspnet: Efficient 6-dof grasp generation in cluttered scenes. In *2021 IEEE international conference on robotics and automation (ICRA)*, pages 13438–13444. IEEE, 2021.

[58] W. Yuan, A. Murali, A. Mousavian, and D. Fox. M2t2: Multi-task masked transformer for object-centric pick and place. In *7th Annual Conference on Robot Learning*, 2023.

[59] B. Sundaralingam, S. K. S. Hari, A. Fishman, C. Garrett, K. Van Wyk, V. Blukis, A. Millane, H. Oleynikova, A. Handa, F. Ramos, et al. Curobo: Parallelized collision-free robot motion generation. In *2023 IEEE International Conference on Robotics and Automation (ICRA)*, pages 8112–8119. IEEE, 2023.

[60] B. Sundaralingam, A. Murali, and S. Birchfield. curobov2: Dynamics-aware motion generation with depth-fused distance fields for high-dof robots. *arXiv preprint arXiv:2603.05493*, 2026.

[61] X. Zhou, Y. Xu, G. Tie, Y. Chen, G. Zhang, D. Chu, P. Zhou, and L. Sun. Libero-pro: Towards robust and fair evaluation of vision-language-action models beyond memorization. *[arXiv preprint arXiv:2510.03827]*, 2025.

[62] H. Minkowski. *Geometrie der Zahlen*. B.G. Teubner, Leipzig, 1896.

[63] W. Shen, C. Garrett, N. Kumar, A. Goyal, T. Hermans, L. P. Kaelbling, T. Lozano-Pérez, and F. Ramos. Differentiable gpu-parallelized task and motion planning. In *Robotics science and systems*. Robotics; Science and Systems, 2025.